

# Structural composites with integrated electromagnetic functionality

Syrus C. Nemat-Nasser, Alireza Vakil Amirkhizi, Thomas Plaisted,  
Jon Isaacs, and Sia Nemat-Nasser\*

## ABSTRACT

We are studying the incorporation of electromagnetic effective media in the form of arrays of metal scattering elements, such as wires, into polymer-based or ceramic-based composites. In addition to desired structural properties, these electromagnetic effective media can provide controlled response to electromagnetic radiation such as RF communication signals, radar, and/or infrared radiation. With the addition of dynamic components, these materials may be leveraged for active tasks such as filtering. The advantages of such hybrid composites include simplicity and weight savings by the combination of electromagnetic functionality with necessary structural functionality. This integration of both electromagnetic and structural functionality throughout the volume of the composite is the distinguishing feature of our approach. As an example, we present a class of composites based on the integration of artificial plasmon media into polymer matrixes. Such composites can exhibit a broadband index of refraction substantially equal to unity at microwave frequencies and below.

## 1. INTRODUCTION

Our work on multifunctional structural composites targets the integration of electromagnetic functionality into lightweight host structures and materials. Our goal is to develop practical models—analytical, computational and experimental—for the design of structural composites with controlled electromagnetic properties. The host composites have advantageous physical properties that we wish to retain while incorporating electromagnetic enhancements such as tunable index of refraction, RF absorption, and in the case of Left-handed materials,<sup>1</sup> negative index of refraction. These electromagnetic enhancements are produced by integrating periodic metal scattering structures with *effective medium* response properties at selectable RF frequencies. Controlled permittivity may be attained from the plasma-like response of periodic inductive structures. The resulting frequency-dependent dielectric constant can be negative or positive. Negative permeability may be attained from periodic arrays of magnetic dipole symmetry resonators such as Pendry's *split-ring resonators*;<sup>2</sup> these resonators display a frequency-dependent magnetic response though they are constructed from non-magnetic conductors such as copper. Negative permeability from split-ring resonator arrays combined with negative permittivity from inductive wire arrays results in a negative index of refraction that occurs in *left-handed media*.<sup>1,3,4</sup> Left-handed media are currently the subject of intense study by our colleagues at UCSD and many others around the world. As a practical matter, the negative refractive response is currently limited to small frequency bands with high RF losses. This manuscript addresses the practical design of structural composites with controlled *positive* index of refraction.

Structured conducting media referred to as *artificial dielectrics* have been studied since the 1950's, and perhaps earlier, for modeling RF propagation in the ionosphere, and due to low their intrinsic losses, these media have also been considered for use as microwave lenses.<sup>5,6</sup> Many artificial dielectrics are plasma analogs that we refer to as *artificial plasmon media*. These example media share an interesting characteristic: they dramatically affect electromagnetic radiation while occupying a small, often negligible volume fraction. In fact, by themselves, the artificial media have little or no structural integrity and are typically held in low-density polystyrene or patterned onto thin plastic sheets, minimizing the contribution of the non-metal components. We are specifically interested in the case where such a medium is embedded in a dielectric matrix with significant structural integrity, forming a *hybrid material* system. Numerical simulations and experiments confirm that the dielectric properties of such hybrid composites do, in the absence of significant RF losses, follow the expected analytical form for the combination of a dilute plasma and an ordinary dielectric material. In particular, we find that such a hybrid material can serve as an RF window (index of refraction  $n \approx 1$ ) over a large bandwidth without significantly altering its other (e.g. structural) properties.

\* Email snematnasser@ucsd.edu; phone 858-534-4772; <http://www-ceam.ucsd.edu>; Center of Excellence for Advanced Materials, UC San Diego, 9500 Gilman Drive, La Jolla, CA, USA, 92093-0416.

## 2. ARTIFICIAL PLASMON MEDIA

The ionosphere is a dilute plasma, and many artificial dielectrics are plasma analogs. In 1996, Pendry et al.<sup>7</sup> presented an *artificial plasmon medium* composed of a periodic arrangement of very thin conducting wires, predicting a plasma frequency in the microwave regime, below the diffraction limit. Recently, other researchers have presented examples of artificial plasmon media at microwave frequencies.<sup>8</sup> The dielectric constant  $\kappa$  of a dilute neutral plasma is given by

$$\kappa = 1 - \left( \frac{f_p^2}{f^2} \right) \quad (1)$$

where  $f_p$  is the *plasma frequency* and  $f$  is the electromagnetic excitation frequency. Thus, a plasma has a dispersive dielectric response. The degree to which an artificial medium obeys Equation 1 must often be determined empirically and depends on the construction materials and on the geometric properties that determine  $f_p$  relative to the inter-element spacing of the metal scattering elements.

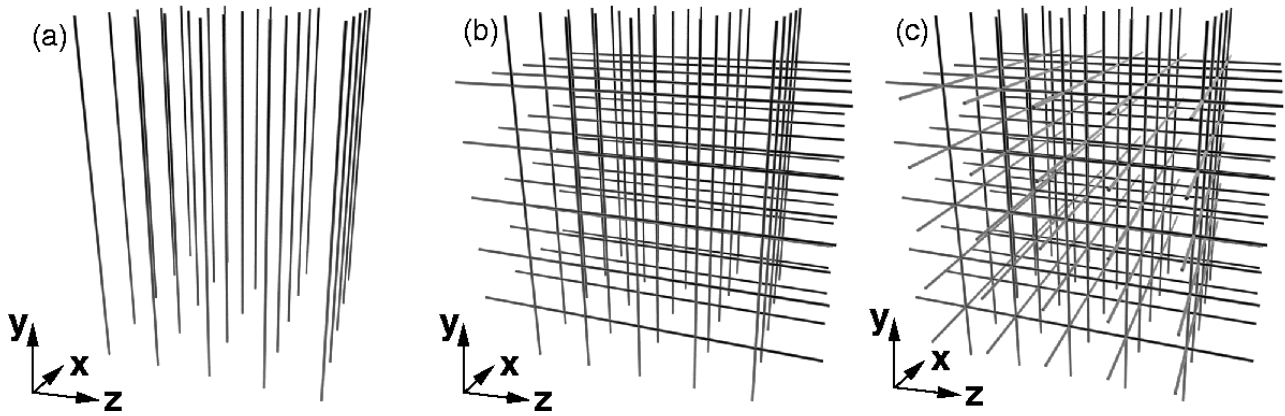


**Figure 1.** Three examples of artificial plasmon media composed of periodic arrangements of straight wires in a square lattice arrangement: (a) two-dimensional medium for electromagnetic radiation with linear polarization along the y-axis; (b) two-dimensional medium for electromagnetic radiation with wave vector  $\mathbf{k}$  parallel to the x-axis and arbitrary polarization; and (c) three-dimensional medium for electromagnetic radiation with arbitrary wave vector and arbitrary polarization. These configurations were considered by researchers in the 1950s<sup>5,6</sup> and recently re-interpreted by Pendry et al.<sup>7</sup> in the 1990s.

We have selected three classes of artificial plasmon media for our research program. We refer to these classes as *thin wire media*, *loop-wire media*, and *coil media*. Thin-wire media, as illustrated in Figure 1, were re-introduced by Pendry et al.<sup>7</sup> in the 1990s who demonstrated through theoretical analysis that these structures can be engineered with a plasma frequency  $f_p$  in the microwave regime, below the diffraction limit. Pendry et al.<sup>9</sup> provide the following prediction for the plasma frequency of a thin wire medium:

$$f_p^2 = \frac{1}{2\pi} \left( \frac{c_0^2/d^2}{\ln\left(\frac{d}{r}\right) - \frac{1}{2}(1 + \ln\pi)} \right) \quad (2)$$

where  $c_0$  is the speed of light in vacuum,  $d$  is the lattice spacing, and  $r$  is the wire diameter.<sup>†</sup> The length of the wires is assumed to be infinite and, in practice, a designer should assure that  $l \gg d \gg r$  where  $l$  is the wire length. Pendry et al.<sup>9</sup> suggest a wire radius of approximately one micron for a lattice spacing of 1cm resulting in a ratio,  $d/r$ , on the order of or greater than  $10^5$ .

Loop-wire media introduced by Smith et al.<sup>8</sup> achieve a microwave frequency plasma frequency though constructed from a relatively thick wire. This is possible due to the observation by Smith that the large effective electron mass calculated

<sup>†</sup> We keep the additional numerical correction factor  $\Delta = -\frac{1}{2}(1 + \ln\pi)$  that Pendry usually drops because we typically employ this formula for values of  $d$  and  $r$  that do not follow the assumption that  $\ln\left(\frac{d}{r}\right) \gg 1$ .

by Pendry is equivalent to an effective inductance of the thin-wire medium. This inductance can be increased by making the wire elements very thin or by arranging inductive loops within the medium. Smith’s loop-wire medium is illustrated in Figure 2. When designing loop-wire or coil media, it is necessary to consider polarization rotation. For example, the two-dimensional coil medium illustrated in Figure 1d will behave like a plasma for linearly polarized electromagnetic radiation. However, the loop-wire medium in Figure 2c will introduce a polarization rotation because all of the loop-wire elements are right-handed.

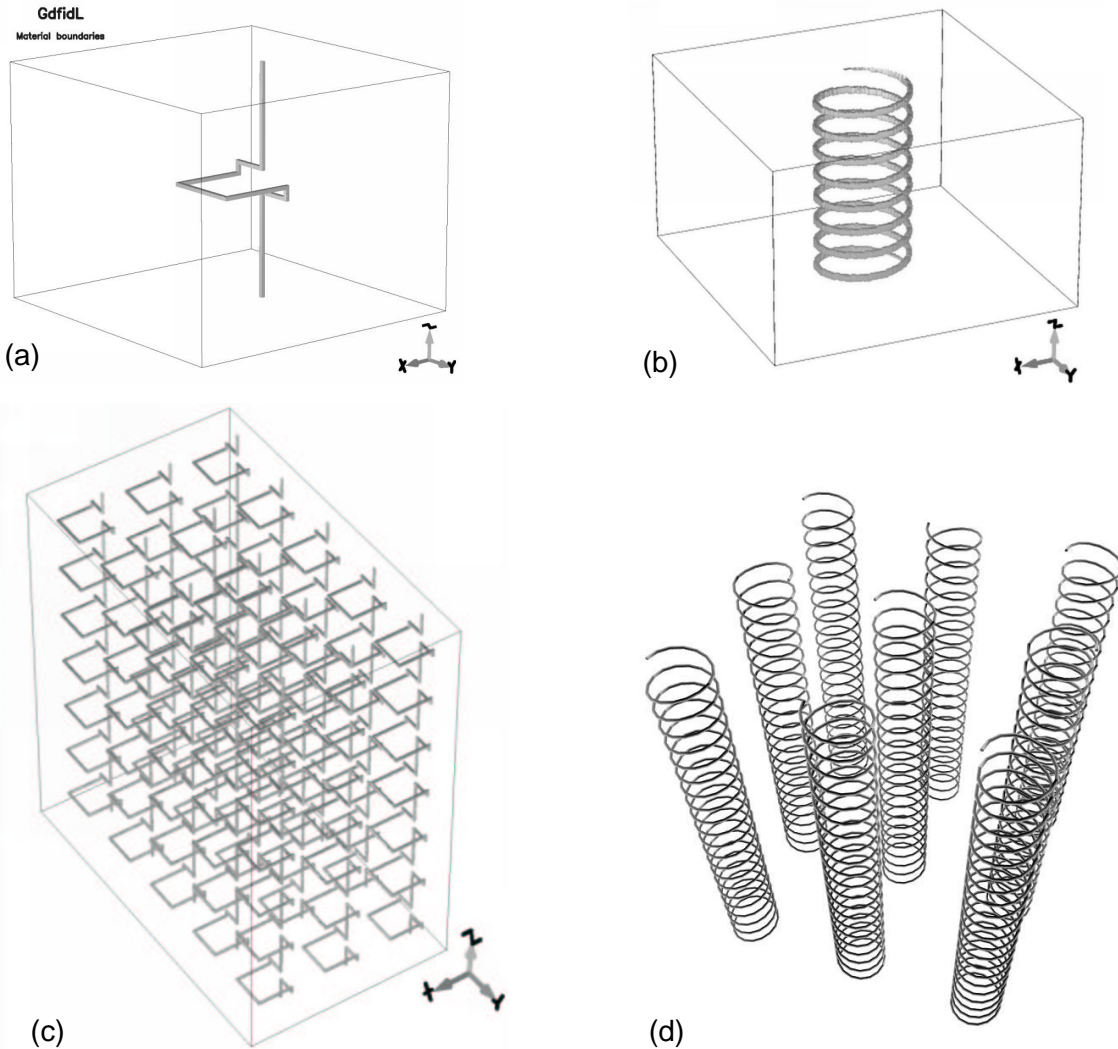


**Figure 2.** The loop-wire medium introduced by Smith et al.<sup>8</sup> and the coil medium that logically follows: (a) A primitive unit cell of a loop-wire medium generated by GdfidL,<sup>10</sup> a finite difference electromagnetic solver; (b) A GdfidL unit cell (not primitive) of a coil medium that represents a maximally inductive extension of the loop-wire unit cell; (c) A finite medium of loop-wire elements, rendered by GdfidL for visual presentation only, that may be compared to the thin wire medium in Figure 1a; and (d) A concept design of a finite coil medium composed of coils with alternating handedness to prevent polarization rotation of linearly polarized electromagnetic radiation.

### 3. PROPERTIES OF PLASMON/POLYMER HYBRID MATERIALS

For a homogeneous conducting medium at low-frequencies, one can express the frequency-dependent dielectric constant as  $\kappa = \kappa_0 + i \frac{\sigma}{\omega \epsilon_0}$ , where  $\sigma$  is the ohmic conductivity of “free” electrons and  $\kappa_0$  is due to the normal dipolar response

of fixed charges.<sup>11</sup> In the case of an ideal plasmon medium, the expression for the dielectric constant follows Equation 1 when the normal dipolar response term is equal to 1 ( $\kappa_0 = 1$ ). In this case, the dielectric constant  $\kappa$  takes on negative values for  $f < f_p$  and asymptotically approaches 1 as  $f \rightarrow \infty$ . The presence of a dielectric matrix (into which the plasmon medium is embedded) will result in a polarization response that can be accounted for by introducing  $\kappa_0$  such that

$$\kappa = \kappa_0 - \left( \frac{f_p^2}{f^2} \right). \quad (3)$$

Now,  $\kappa$  is the *effective dielectric constant* of an ideal plasmon/dielectric composite material. The dipolar response term  $\kappa_0$  is substantially equal to the effective dielectric constant of the polymer composite matrix in the absence of the integrated artificial plasmon medium when that medium closely obeys Equation 1 and also occupies a negligible volume fraction of the composite. With the addition of the dielectric host matrix, the dielectric constant  $\kappa$  takes a value of unity at a finite frequency  $f_1 = f_p/\sqrt{\kappa_0 - 1}$ . We will refer to  $f_1$  as the *match frequency*, the frequency at which  $\kappa = 1$ , the index  $n = 1$ , and there is no refraction at an interface between air and the ideal composite material. The frequency at which  $\kappa = 0$  determines the onset of electromagnetic wave propagation. This *turn-on frequency* is given by  $f_0 = f_p/\sqrt{\kappa_0}$ . Figure 3 illustrates the dependence of  $f_0$  and  $f_1$  on the matrix dielectric constant.

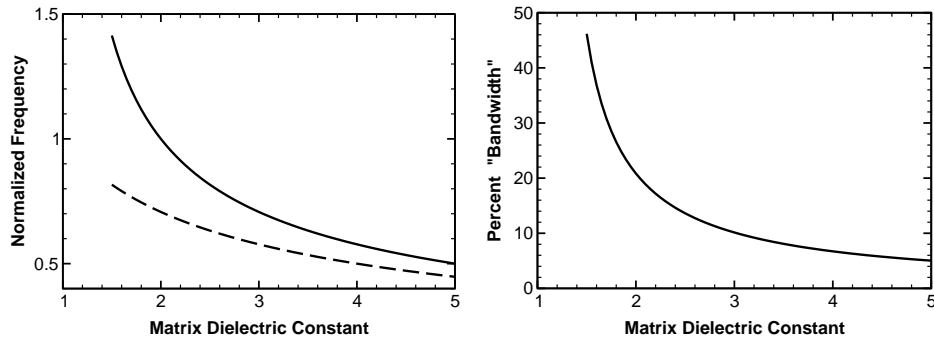


**Figure 3.** Illustration of the dependence of the effective dielectric properties of plasmon/polymer hybrids on the host matrix dielectric constant: [Left] The *turn-on frequency*  $f_0$  (dashed line) and *match frequency*  $f_1$  (solid line) as a function of the matrix dielectric constant  $\kappa_0$  where the normalized frequency is in units of the plasma frequency  $f_p$ ; and [Right] A type of *bandwidth* as a function of the matrix dielectric constant  $\kappa_0$ . This percent *bandwidth* is defined as  $(f_{n=1.1} - f_{n=0.9})/f_1$ . It illustrates the increased dispersion around  $n = 1$  as  $\kappa_0$  increases.

#### 4. COMPOSITES WITH INTEGRATED ARTIFICIAL PLASMON MEDIA

The conditions for an ideal plasmon/dielectric composite are that electromagnetic losses may be neglected and that the effective medium approximation is valid. For this, the electromagnetic wavelength  $\lambda$  must be much larger than the lattice spacing of the artificial plasmon medium. Because we are interested in index of refraction close to unity, we may compare the free space wavelength  $\lambda_0 = c_0/f$  to the scattering medium lattice spacing. Figure 4 presents three laboratory prototypes of plasmon polymer hybrids. These include a loop-wire medium constructed on a two-dimensional array of threaded nylon rods; a thin wire medium in a block of Rexolite, a cross-linked polystyrene material with favorable RF properties; and a coil medium held under tension within a two-dimensional array of holes in a polymer material.

Our first hybrid material prototype was actually a hybrid structure of threaded nylon rods that supported a loop-wire artificial plasmon medium; see Figure 4a. This structure was designed through numerical simulations of electromagnetic wave propagation. These simulations were performed with GdfidL,<sup>10</sup> an electromagnetic solver developed by Dr. Warner Bruns. The geometry represented in Figure 2a was used with the addition of a nylon rod component, representing the structure shown in Figure 4a. To simplify the simulation, a square geometry, with equivalent cross-sectional areas, was used for both the loop-wire element and the nylon rod. With GdfidL, we performed a finite difference frequency domain (FDFD) calculation of the dispersion for the nylon rod structure. The calculated dispersion provides the mode frequency

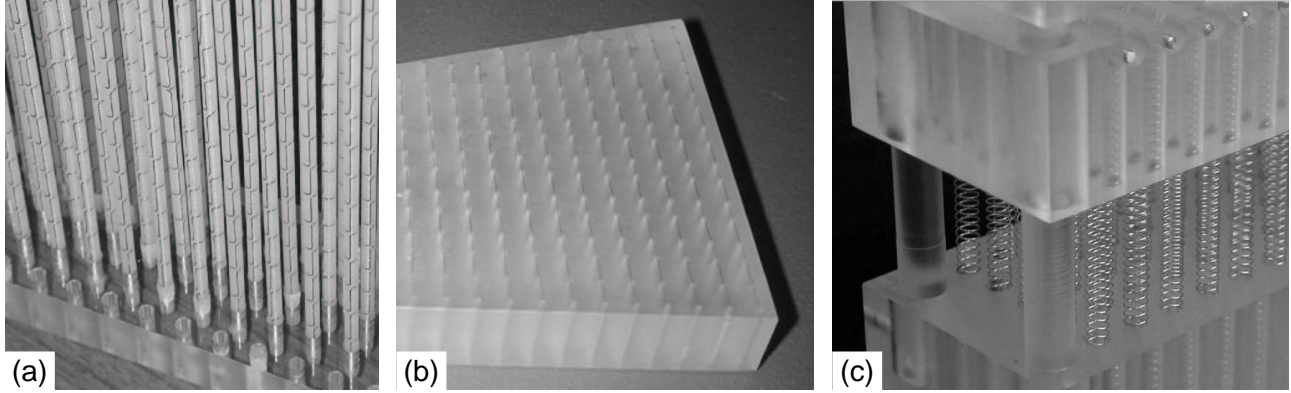


**Figure 4.** Laboratory scale prototypes of plasmon polymer hybrids: (a) A copper loop-wire medium (see Figure 2) incorporated into a lattice of 6-32 threaded nylon rods. The threaded rods were scored along their length to provide a wire guide, and the threads were used support and position the inductive loops; (b) A thin wire medium (see Figure 1a) of  $50\mu\text{m}$  diameter copper wire integrated into a two-dimensional square lattice of holes in a polymer material. This thin sample is designed to be placed between two metal plates that make electrical contact with each of the wires. The resulting configuration simulates an infinite material in the direction perpendicular to the plates. Such two-dimensional guided wave measurements are discussed by Shelby et al.<sup>4</sup> and Smith et al.<sup>12</sup>; (c) A coil medium with coils of alternating sense (see Figure 2d) incorporated into a square array of holes in a polymer matrix. The coils are held in tension and are mechanically adjustable by variation of their overall length.

as a function of phase advance across the unit cell in the direction of wave propagation, the x-direction in Figure 2a. The wave number  $k$ , the magnitude of the electromagnetic wave vector  $\mathbf{k}$ , is directly related to the phase advance  $\phi$ , measured in radians, and the size of the unit cell  $d$ , as  $k = \phi/d$ . The predicted index of refraction may thus be extracted from the GdfidL calculation as

$$n = \frac{kc_0}{2\pi f} = \frac{\phi c_0}{2\pi f d}, \quad (4)$$

where  $f$  is the mode frequency of the GdfidL solution and  $c_0$  is the speed of light in vacuum. The results of the GdfidL calculation and a confirming experiment are presented in Figure 5.

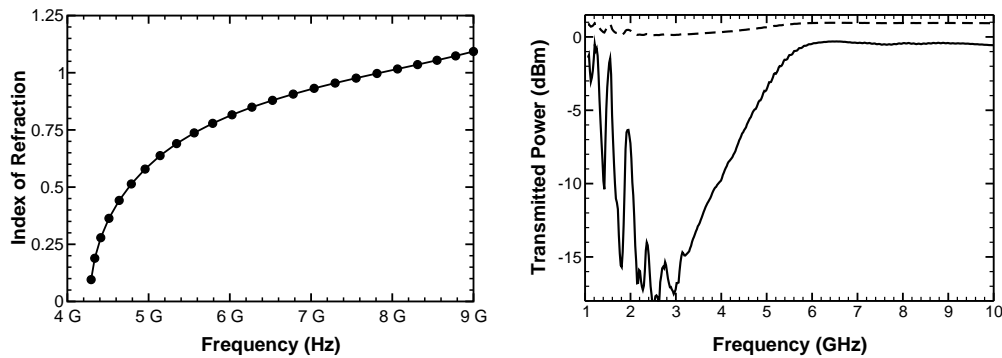


**Figure 5.** Computational analysis and experimental confirmation of a loop-wire plasmon medium combined with a periodic lattice of nylon rods as shown in Figure 4a. [Left] Predicted index of refraction from GdfidL simulations of an infinite medium based on the unit cell similar to Figure 2a. [Right] Results of power transmission measurements of a finite structure three rows thick with approximate dimensions of  $12 \times 12 \times 1\text{in}^3$ . The sample filled an aperture in a wall of radar absorbing material (RAM) for the transmission measurement (solid line), and a reference measurement (dashed line) was made through the empty aperture. The predicted turn-on frequency  $f_0$  from the simulation is approximately 4.3GHz and correlates well to the turn-on of propagation seen in the transmission measurement. This measurement was performed for us by W. Massey and D. Hurdsmann at the SPAWAR Systems Center San Diego.

Figure 6 illustrates a validation of Equation 2 for the plasma frequency and Equation 3 for the resulting effective dielectric constant of a thin wire artificial plasmon medium embedded in a solid polymer matrix. Applying the prediction for  $f_p$  and the known dielectric constant of Rexolite  $\kappa_0 = 2.5$  to Equation 3, we designed a plasmon polymer hybrid with a predicted turn-on frequency  $f_0 = 7.8\text{GHz}$  and a predicted match frequency  $f_1 = 10\text{GHz}$ . We characterized this sample with an angular resolved microwave transmission measurement developed by Richard Shelby in the laboratory of Professor S. Schultz at UCSD.<sup>4</sup> This measurement employs a microwave beam guided between closely spaced metal plates; the electric field of this guided beam is constrained by the geometry such that the electric field component is spatially uniform along any perpendicular projection between these plates. For a plasmon sample such as our plasmon polymer hybrid, the measurement requires electrical contact between the metal guide plates and each of the wires. In this measurement, the distance between the sample and the microwave detector (see Figure 6a) was shorter than that required to avoid Fresnel effects. The lattice spacing  $d$  of the plasmon medium was approximately 5mm. Given the RF wavelength  $\lambda = 3\text{cm}$  at 10GHz, this hybrid was not an ideal example of a plasmon polymer hybrid because the wavelength to lattice spacing ratio  $\lambda/d = 6$  was not sufficiently large. Despite these limitations, both the predicted turn-on frequency  $f_0$  and the match frequency  $f_1$  were remarkably consistent with the measurements.

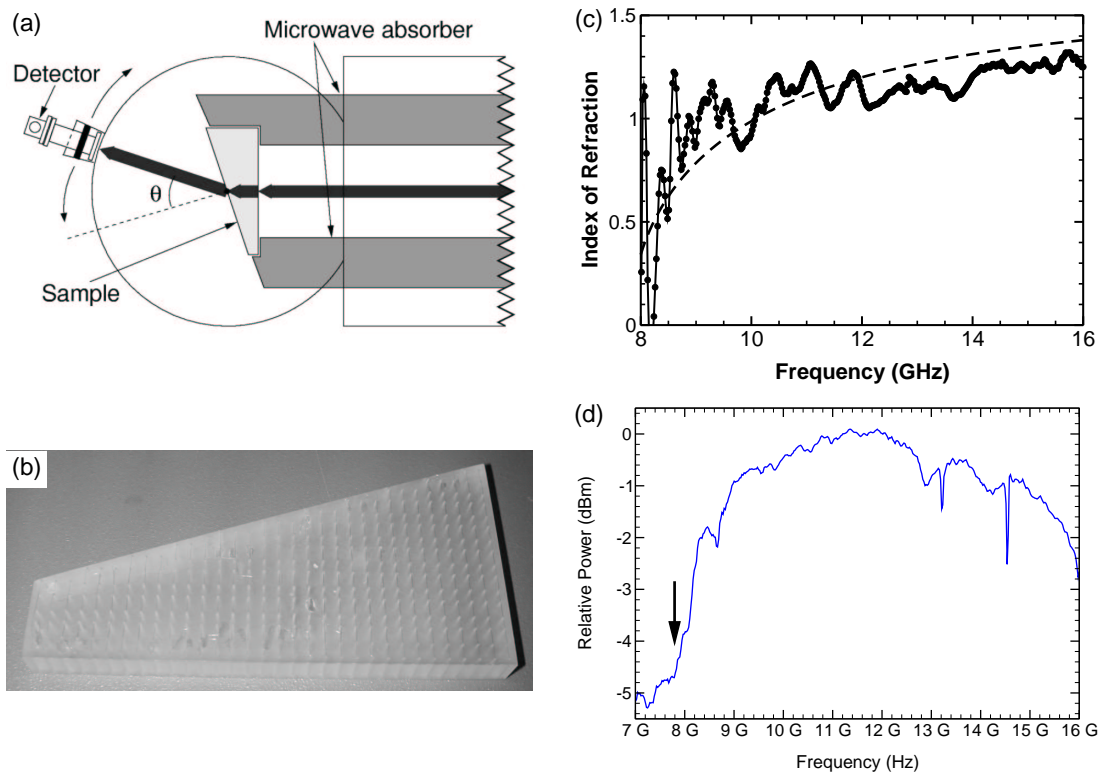


**Figure 6.** Experimental confirmation of Equation 2 and Equation 3: (a) Schematic of measurement apparatus developed by R. Shelby [figure reproduced from Shelby et al.<sup>4</sup>] for confirmation of negative index of refraction. The refraction angle  $\theta$  shown here indicates a positive index of refraction; (b) A polymer wedge-shaped sample with integrated thin wire plasmon medium made of  $50\mu\text{m}$  diameter copper wire arranged in a square two-dimensional lattice with lattice spacing  $d \sim 5\text{mm}$  (see Figure 1a). The polymer employed is Rexolite, a cross-linked polystyrene material with dielectric constant  $\kappa_0 \simeq 2.5$  and very low dielectric loss tangent. Equation 2 was used to predict the plasma frequency  $f_p$  for the thin wire medium; (c) The measured index of refraction (solid line with filled circles) along with the prediction that follows from Equation 3 (dashed line); (d) The relative transmitted power through the plasmon wedge as a function of frequency. The predicted turn-on frequency, indicated by an arrow, is 7.8GHz according to Equation 3.

To consider a better example of an ideal effective medium hybrid, we modeled a coil medium such as that shown in Figure 2 with a plasma frequency  $f_p \sim 1.4\text{GHz}$  corresponding to a free-space wavelength  $\lambda = 21\text{cm}$ . With a lattice spacing of 1cm, this medium has  $\lambda/d \sim 20$ . We studied the validity of Equation 3 for this medium using a series of simulations

where the host matrix dielectric constant  $\kappa_0$  was varied. The results appear in Figure 7.

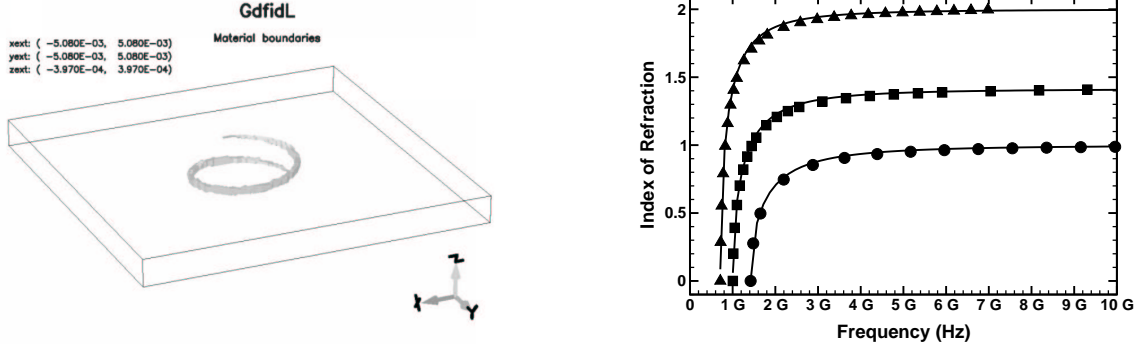


**Figure 7.** Computational confirmation of Equation 3 for a two-dimensional coil medium (see Figure 2) embedded in a host dielectric matrix with dielectric constant  $\kappa_0$ . [Left] GdfidL<sup>10</sup> unit cell for the simulation of RF propagation in an infinite two-dimensional periodic lattice. [Right] Simulated index of refraction versus frequency: Solid lines represent the theoretical prediction of Equation 3. The shapes represent GdfidL simulations of the index of refraction as a function of frequency for  $\kappa_0 = 1$  (filled circles),  $\kappa_0 = 2$  (filled squares), and  $\kappa_0 = 4$  (filled triangles).

## 5. EFFECTIVE DIELECTRIC CONSTANT OF COMPOSITES

The artificial plasmon medium is embedded in a fiber reinforced composite host that is designed for optimal thermo-mechanical attributes to provide necessary stiffness, strength, toughness, and thermal management. The overall thermo-mechanical as well as electromagnetic properties of such a host composite can be estimated using various micro-mechanical models; see Nemat-Nasser and Hori.<sup>13,14</sup> Here we focus on estimating the effective dielectric tensor,  $\kappa_0$ , of the host composite, considering for illustration a two-phase material, e.g., polymer matrix phase (denoted by subscript 1) containing reinforcing fibers (denoted by subscript 2).

The effective dielectric constant of this two-phase composite can be expressed as<sup>13</sup>

$$\kappa_0 = (1 - c)\kappa_1\mathbf{A}_1 + c\kappa_2\mathbf{A}_2 \quad (5)$$

where  $\kappa_1$  and  $\kappa_2$  are the dielectric tensors of phase 1 and 2,  $\mathbf{A}_1$  and  $\mathbf{A}_2$  are the corresponding field concentration tensors, and  $c$  is the volume fraction of phase 2. The concentration tensors are defined by

$$\langle \mathbf{E}_1 \rangle = \mathbf{A}_1\mathbf{E}^0, \quad \langle \mathbf{E}_2 \rangle = \mathbf{A}_2\mathbf{E}^0, \quad (1 - c)\mathbf{A}_1 + c\mathbf{A}_2 = \mathbf{I} \quad (6)$$

where  $\langle \mathbf{E} \rangle$  denotes the volume average of  $\mathbf{E}$ ,  $\mathbf{E}^0$  is the electric field applied at the boundary, and  $\mathbf{I}$  is the second-order unit tensor. If these concentration tensors are set equal to the unit tensor, then one obtains the results originally proposed by Voigt.<sup>15</sup> It is clear that the effectiveness of the model depends on the effectiveness of the estimate of these concentration tensors.

It is also possible to start with estimating the inverse of the electric permittivity,  $\kappa_0^{-1} = \mathbf{R}_0$ , in terms of the corresponding constituent parameters as

$$\mathbf{R}_0 = (1 - c)\mathbf{R}_1\mathbf{B}_1 + c\mathbf{R}_2\mathbf{B}_2 \quad (7)$$

where  $\mathbf{B}$ 's are now the concentration tensors. We shall not follow this line of calculation here and refer the reader to Nemat-Nasser and Hori<sup>13</sup> for details. Here, we use a simple model to calculate explicitly the concentration tensors,  $\mathbf{A}_1$  and  $\mathbf{A}_2$ , adopting a special version of the double-inclusion model proposed by Nemat-Nasser and Hori.<sup>13</sup> To this end, we assume that the average field,  $\langle \mathbf{E}_2 \rangle$ , in phase 2, is equal to the average field in a single inclusion embedded in an infinite homogeneous matrix subjected to an external field equal to the yet-unknown average field,  $\langle \mathbf{E}_1 \rangle$ , in phase 1,

$$\langle \mathbf{E}_2 \rangle = \mathbf{A}_2^{dil} \langle \mathbf{E}_1 \rangle, \quad \mathbf{A}_2^{dil} = [\mathbf{I} + \mathbf{S}\kappa_1^{-1}(\kappa_2 - \kappa_1)]^{-1}, \quad (8)$$

where  $\mathbf{A}^{dil}$  is a concentration tensor for the dilute distribution of phase 2 inclusions (*i.e.*, no interaction with other inclusions), and can be determined, using Eshelby's equivalent-inclusion concept,<sup>16</sup> for an assumed inclusion geometry. In the second expression above,  $\mathbf{S}$  is the dielectric Eshelby tensor. For example, with a spherical inclusion embedded in an isotropic matrix (Taya and Arsenault<sup>17</sup>),  $S_{11} = S_{22} = S_{33} = \frac{1}{3}$ . From the above expressions, we now obtain

$$\mathbf{A}_2 = \mathbf{A}_2^{dil} [(1 - c)\mathbf{I} + c\mathbf{A}_2^{dil}]^{-1}. \quad (9)$$

For spherical inclusions, in particular, we obtain, after some manipulation,

$$\kappa_0 = \frac{\kappa_1 + \kappa_2 - c(\kappa_1 - \kappa_2)}{\kappa_1 + \kappa_2 + c(\kappa_1 - \kappa_2)} \kappa_1 \quad (10)$$

where the constituents and the resulting composite are assumed to be isotropic. Similar results can be obtained for other geometries of the inclusions. Also, in many applications a periodic microstructure may better correspond to the actual fiber arrangement. Again, the concentration tensors can be calculated and the procedure remains the same. For these cases as well as for finite composites, it is possible to obtain explicit lower and upper bounds on the effective electric permittivity, as discussed in Nemat-Nasser and Hori.<sup>14</sup>

## 6. CONCLUSION

We have presented analytical and numerical models for the electromagnetic enhancement of structural composites. This enhancement, in the form of integrated conducting media such as artificial plasmon media, can be used to control RF properties such as the index of refraction in a desired frequency band. Through computational analysis and experimental characterization of laboratory-scale prototypes, we have demonstrated our capability to design hybrid composites based on models such as those represented by Equations 2, 3, and 10.

## Acknowledgments

The authors wish to thank Leo Christodoulou (DARPA) and John Venables (IDA) for their continued encouragement and many stimulating discussions. We also thank: David R. Smith and Sheldon Schultz for useful conversations and access to their microwave characterization facilities; Richard Shelby for help with microwave measurements of refractive index; W. Massey, J. Meloling, D. Hurdsman, and J. Rockway for microwave characterization measurements performed at their expense at the SPAWAR Systems Center San Diego. This research is supported by ARO DAAD19-00-1-0525 to the University of California, San Diego.

## References

1. D.R. Smith, W.J. Padilla, D.C. Vier, S.C. Nemat-Nasser, and S. Schultz. Composite medium with simultaneously negative permeability and permittivity. *Physical Review Letters*, 84(18):4184–7, 2000.
2. J.B. Pendry, A.J. Holden, D.J. Robbins, and W.J. Stewart. Magnetism from conductors and enhanced nonlinear phenomena. *IEEE Transactions on Microwave Theory and Techniques*, 1999.
3. R.A. Shelby, D.R. Smith, S.C. Nemat-Nasser, and S. Schultz. Microwave transmission through a two-dimensional isotropic left-handed metamaterial. *Applied Physics Letters*, 78(4):489–491, 2001.
4. R.A. Shelby, D.R. Smith, and S. Schultz. Experimental verification of a negative index of refraction. *Science*, 292(5514):77–9, April 2001.
5. R.N. Bracewell. Analogues of an ionized medium. *Wireless Engineer*, 31:320–6, December 1954.
6. W. Rotman. Plasma simulation by artificial dielectrics and parallel-plate media. *IRE Transactions on Antennas and Propagation*, pages 82–95, January 1962.
7. J.B. Pendry, A.J. Holden, W.J. Stewart, and I. Youngs. Extremely low frequency plasmons in metallic mesostructures. *Physical Review Letters*, 76(25):4773–6, 1996.
8. D.R. Smith, D.C. Vier, W. Padilla, S.C. Nemat-Nasser, and S. Schultz. Loop-wire medium for investigating plasmons at microwave frequencies. *Applied Physics Letters*, 75(10):1425–7, 1999.



9. J.B. Pendry, A.J. Holden, D.J. Robbins, and W.J. Stewart. Low frequency plasmons in thin-wire structure. *J. Phys.: Condens. Matter*, 10:4785–4809, 1998.
10. W. Bruns. Gdfidl: A finite difference program for arbitrarily small perturbations in rectangular geometries. *IEEE Transactions on Magnetics*, 32(3):1453–1456, May 1996.
11. J.D. Jackson. *Classical Electrodynamics*. Wiley, 1975.
12. D.R. Smith, R. Dalichaouch, N. Kroll, S. Schultz, and P.M. McCall, S.L. and Platzman. Photonic band structure and defects in one and two dimensions. *Journal of the Optical Society of America B*, 10(2):314–21, 1993.
13. S. Nemat-Nasser and M. Hori. *Micromechanics: Overall Properties of Heterogeneous Materials*, volume 37 of *North-Holland series in applied mathematics and mechanics*. North-Holland, Amsterdam ; New York, first edition, 1993.
14. S. Nemat-Nasser and M. Hori. *Micromechanics: Overall Properties of Heterogeneous Materials*. Elsevier, North-Holland, second revised edition, 1999.
15. W. Voigt. *Lehrbuch der Kristallphysik*. Teubner, Leipzig, 1889.
16. J.D. Eshelby. The determination of the elastic field of an ellipsoidal inclusion and related problems. *Proceedings of the Royal Society of London, Series A*, 241:376–396, 1957.
17. M. Taya and R.J. Arsenault. *Metal matrix composites : thermomechanical behavior*. Pergamon Press, Oxford, England; New York, 1989.